

Performance comparison of MLP and RBF neural networks to predict CO emissions of a spark ignition gasoline engine

José D. Martínez-Morales*. Elvia R. Palacios-Hernández**. Jorge A. Morales-Saldaña***

*Autonomous University of Campeche, 24039 México
(Tel: 4448035711; e-mail: jdmartinez.morales@gmail.com)

**Faculty of Science, Autonomous University of San Luis Potosí, 78290, México

***Faculty of Engineering, Autonomous University of San Luis Potosí, 78290, México

Abstract: In this work, a radial basis function (RBF) and multilayer perceptron (MLP) neural networks are compared in order to predict the carbon monoxide emission (CO) of an internal combustion engine. The prediction of CO emissions is performed over several operating conditions defined by the engine speed and the angle of throttle valve. The prediction of the CO emission is determined by four parameters considered as inputs into the input layer of the neural networks. Whereas that the output response of engine that was measured at the exhaust tile pipe is carbon monoxide (CO). Performances of the different predictor models are evaluated using the correlation coefficient R^2 and the mean absolute percentage error (MAPE). The results showed that the use of RBF neural network can describe the emission behavior of the studied gasoline engine in a more precise manner with correlation coefficient R^2 between the measured and predicted CO of 0.9306, whereas that, with the MLP neural network is obtained a correlation coefficient of $R^2 = 0.86558$.

Keywords: artificial neural network, internal combustion engine, radial basis function.

1. INTRODUCTION

Internal combustion engines of modern vehicles release tons of greenhouse gases into the atmosphere each year, as nitrogen oxides (NO_x), hydrocarbons (HC), particulate matter (PM), and additionally carbon monoxide (CO). Limits of the amount of pollutants that can be released into the environment have been imposed by governments, as the new European driving cycle (NEDC) which is a driving cycle designed to assess the emission levels of vehicle engines. In order to reduce exhaust emissions of an internal combustion engine is necessary to recalibrate the electronic control unit, which contains look-up tables for a driving cycle (Guerrier et al. 2004). A manual calibration at the engine test bench is a very demanding task of time and resources. So it is best to have a computer model of the engine and carry out the calibration offline in the PC and then upload the new values of the operating parameters to the ECU.

Some models have been developed to explain the phenomena inside of an internal combustion engine (Kim et al. 2001, Rakopoulos et al. 2008, Pitsch et al. 1996). However, recently artificial neural networks (ANN) have been used in order to modeling nonlinear behavior in various topics of engineering, including modeling of internal combustion engine performance (Thompson et al. 2000, Kiani et al. 2010, Martínez-Morales et al 2013, Martínez-Morales et al. 2014). Adam et al. (2017) designed a physics-based, control-oriented model for

commercial vehicle diesel engines equipped with a high pressure EGR system and exhaust throttle. Hao et al. (2012) proposes different models for estimation of NO_x emissions, in particular, the performance of ACO-SVR model were compared to those of both BPNN and GRNN model, with 92% of cases in test data had the relative error smaller than 5%. Martínez-Morales et al. (2013) proposed wavelet neural network to predict HC, CO and NO_x exhaust emissions, values R^2 of 0.9714, 0.9626 and 0.9929 were observed respectively, between the measured and estimated emissions. Yiran et al. (2015) used a RBF network to predict the dynamics of air manifold and fuel injection in spark ignition engines. Martínez-Morales et al. (2014) proposed RBF and LOLIMOT neural networks to modelling NO_x emissions obtaining $R^2 = 0.97979$ y $R^2 = 0.99452$ respectively. Harisankar et al. (2016) used a set of experimental data obtained from the ethanol HCCI engine to characterize variations in performance measures such as brake thermal efficiency, and exhaust gas temperature, and the emission parameters such as unburned hydrocarbons (UHC), carbon monoxide (CO), nitric oxide (NO), and smoke opacity by means a neural network, trained, validated and tested with experimental data sets. Mohammadhassani et al. (2015) combine artificial neural network (ANN) and ant colony optimization (ACO) to modeling and reducing NO_x and soot emissions from a direct injection diesel engine, with the correlation factors of 0.98 and 0.96, respectively. In particular, the structure of ANN enables them to model

complex nonlinear multiple problems, which makes them an appropriate method for pollutant modeling. In this work, ANN modeling was used to predict CO exhaust emissions in a gasoline engine through of the engine operating parameters.

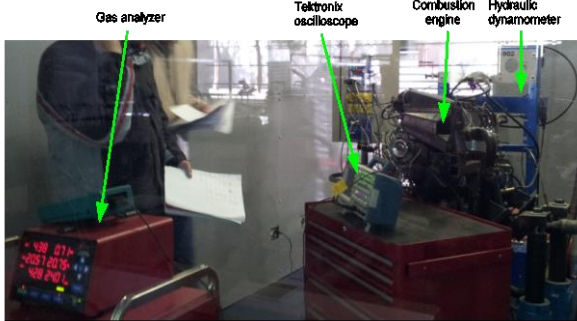


Fig. 1. Experimental apparatus of the engine test bench

2. Experimental setup

In Fig. 1 is shown the engine test-bench used in this work, it consists of a dynamometer connected with the crankshaft of the engine to control the load torque in real time. Carbon monoxide exhaust emission is measured in static mode in the engine, for different values of operating parameters as engine angular speed in revolutions per minute (n_{eng} in rpm), injection time in milliseconds (t_{inj} in ms), the injected fuel mass flow (m_{fuel} in lb/hr) and the angle of the admission throttle valve (α_{th} in %). In Table 1 are shown the characteristics of the studied internal combustion engine.

Table 1. Characteristics of the gasoline engine

Characteristic	Value
Model	Z16SE 2005
Maximum power	100 Hp/5600 rpm
Displacement	1.597 L
Stroke	81.5 mm
Compression ratio	9.4:1
Injection type	Secuential
Maximum Torque	138 Nm/3200 rpm

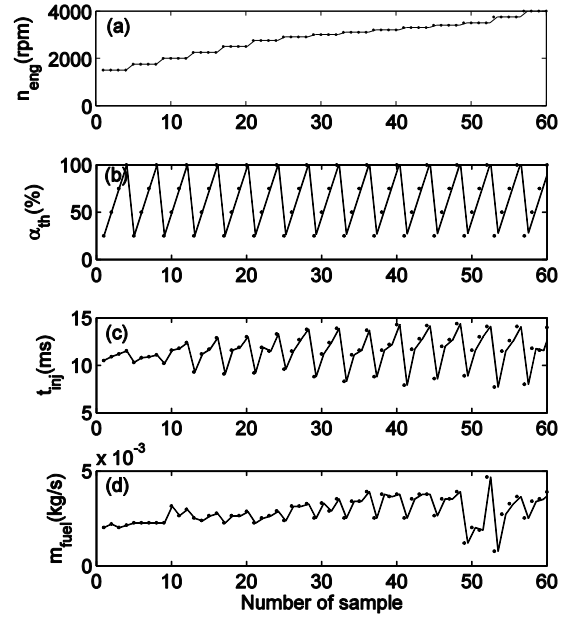


Fig. 2. Input data for training and test ANN; (a) engine speed (b) angle of throttle valve (c) injection time (e) injected fuel mass flow.

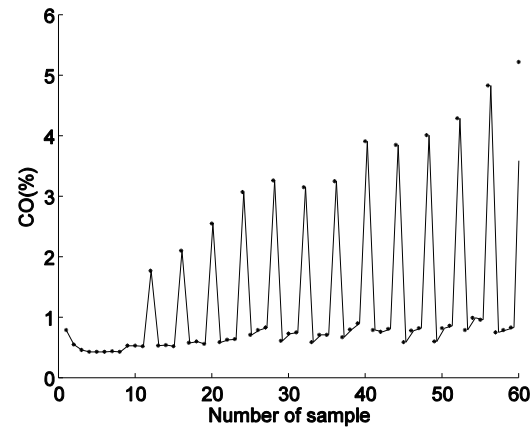


Fig. 3. Output data of CO emission for training and testing ANN.

The gasoline engine is tested over four angles of the admission throttle valve for 15 engine speed values, is that, a total of 60 operating points are established to acquire the values of CO emissions. The taken values of engine speed are $n_{eng} = \{1500, 1750, 2000, 2250, 2500, 2750, 2900, 3000, 3100, 3200, 3300, 3400, 3500, 3750, 4000\}$. Moreover, the operating parameters t_{inj} , and m_{fuel} stored for all the 60 operating conditions. The gas analyzer type FGA4000XDS is used to measure CO exhaust emissions, the injected fuel mass flow m_{fuel} is measured by the software of the Super Flow SF-902 hydraulic dynamometer, which is used to provide load to

the engine. The time of the open state of an injector t_{inj} , is measured by a Tektronix oscilloscope. Sample data of combustion engine are shown in Fig. 2 and 3.

3. Prediction of CO emission

3.1 Radial basis function neural network

A RBF network consists of an input layer determined by the inputs to the network. A hidden layer applies a non linear transformation to inputs. And the output layer, which applies a linear transformation to produce the network output (Simpson et al. 1990). The activation

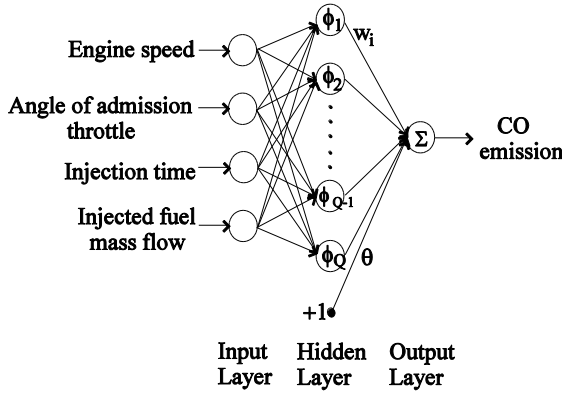


Fig. 4. Structure for the RBF neural network to predict CO emission.

function is a radial basis function defined as

$$\phi(x, c) = \exp\left(\frac{-\|x - c\|^2}{2\sigma^2}\right) \quad (1)$$

where $x = (x_1, x_2, \dots, x_p)^T$ is the vector of p inputs, c are the centers and σ are the widths of the radial function. The RBF network uses a sum of products to compute the outputs. The prediction of a RBF network with Q neurons in the hidden layer is given by

$$y_{pred} = \sum_{i=1}^Q w_i \phi_i(x, c) \quad (2)$$

where w_i denotes the i th weight for each neuron in the hidden layer. To construct RBF network, the number of neurons in the hidden layer must be set, and the centers c , the widths σ and the weights w_i must be estimated. In RBF typical learning, the network structure will be determined using the least mean squared method. In Fig. 4 is shown the structure of a RBF neural network to predict CO emission.

3.2. Multilayer perceptron neural network

The MLP neural network used in this work consists of an input layer, one hidden layer with Q neurons and one

output layer, the activation of the i th hidden neuron, $i = 1, 2, \dots, Q$, is given by

$$u_i = \sum_{j=1}^p w_{ij} x_j + \theta_i \quad (3)$$

where w_{ij} is the weight connecting the j th input unit to the i th hidden neuron, θ_i is the bias of the i th hidden neuron and x_j is the j th input variable, $j = 1, 2, \dots, p$. The output of the i th hidden neuron is defined as

$$y_i = \phi_i(u_i) = \phi_i\left(\sum_{j=1}^p w_{ij} x_j + \theta_i\right) \quad (4)$$

where $\phi_i(\cdot)$ is the activation function. Therefore, the output values of the output neuron are given by

$$y_{pred} = \phi\left(\sum_{i=1}^Q m_i y_i + b\right) \quad (5)$$

where m_i is the weight connecting the i th hidden neuron to the output neuron, and b is the threshold of the output neuron. The activation function used for this neural network is Log-Sigmoid, therefore the output of this network is calculated as follows

$$y_{pred} = \frac{1}{1 + e^{-\sum_{i=1}^Q m_i y_i + b}} \quad (6)$$

A neural network needs to be trained before importing testing datasets. Different algorithms are available to train neural networks, in this work, MLP neural network is trained by adjusting the weights using the Levenberg-Marquardt algorithm which is used to solve predicting problems. It provides an efficient learning procedure for

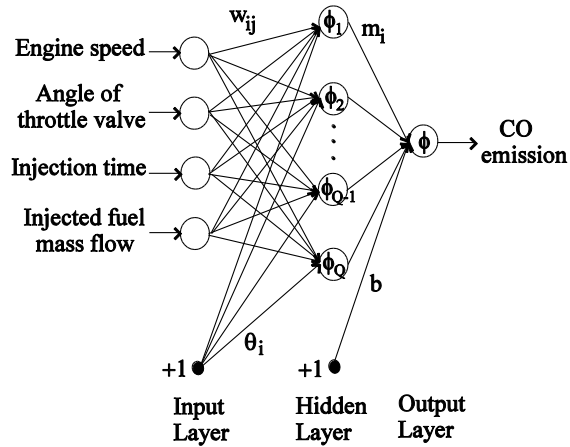


Fig. 5. Structure for the MLP neural network to predict CO emission.

multilayer neural networks. Fig. 5 depicts the structure of the MLP neural network used.

4. Performance criteria

Sixty samples are collected for each input and the output variable, this datasets are divided into training and testing datasets. Among the total datasets, 40 are chosen for training of the models, while the reminding 20 are used as validation data of the models. Once the different stages of the training process had been performed, it is important to estimate the ANN prediction qualities in order to determine a suitable architecture of models and validate these. For this, datasets that are not used for training networks are chosen. The ANN response is assessed using different standard statistical performance evaluation criteria. The statistical measure considered here, is the mean absolute percentage error (MAPE) and the correlation coefficient (R^2). MAPE performance is calculated as

$$MAPE = \frac{1}{T} \left[\sum_{i=1}^T \left| \frac{y_{meas_i} - y_{pred_i}}{y_{meas_i}} \right| \right] \times 100 \quad (7)$$

where $T = 20$ is the number of test datasets, y_{meas_i} is measured value and y_{pred_i} is predicted value by the neural model over all test dataset. Furthermore, the error arose during testing in each model can be expressed as absolute fraction of variance as

$$R^2 = 1 - \left(\frac{\sum_{i=1}^T (y_{meas_i} - y_{pred_i})^2}{\sum_{i=1}^T (y_{pred_i})^2} \right) \quad (8)$$

The optimal values of the number of neurons of the hidden layer for each ANN model is obtained by trial and error method based on these performance criteria. Figure 6 shows the MAPE for the testing data when the number of hidden neurons is increasing for RBF neural network. Here, smaller value of MAPE is obtained with

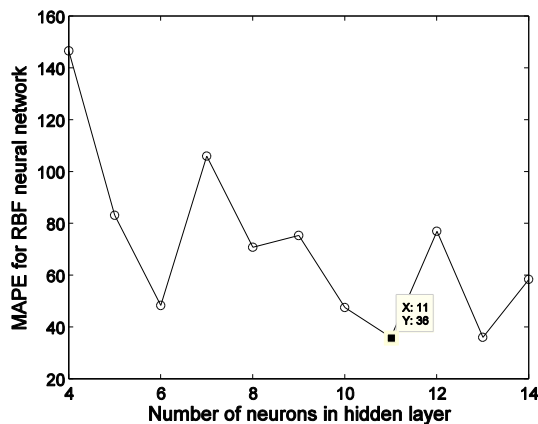


Fig. 6. MAPE behavior for different number of neurons in the hidden layer for RBF ANN

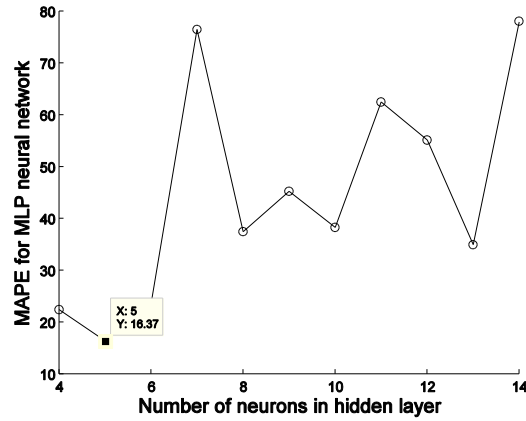


Fig. 7. MAPE behavior for different number of neurons in the hidden layer for MLP ANN.

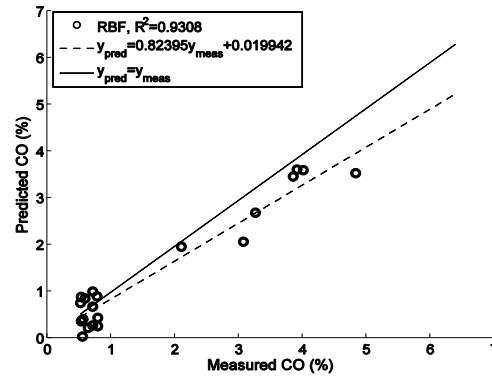


Fig. 8. Correlation coefficient R^2 for CO with RBF neural network.

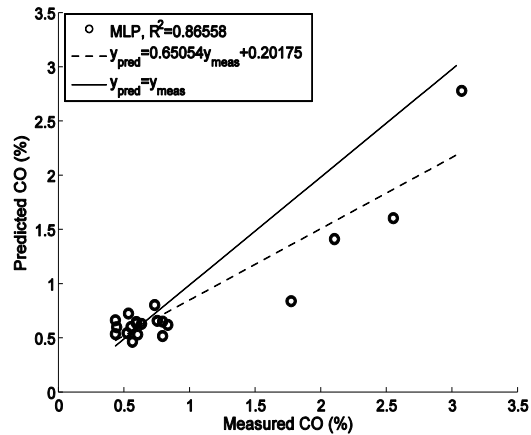


Fig. 9. Correlation coefficient R^2 for CO with MLP neural network.

architecture (6,13,1). Whereas that the behavior of MAPE varying the number of hidden neurons is shown in Fig. 7 for MLP neural network. In this case the MAPE is smaller with architecture (6,5,1) for CO modeling. Finally, in Fig.

8 and 9 are shown the correlation between recorded and predicted exhaust emission by using RBF and MLP network architectures with minimum MAPE respectively. In these Figures it is visible that the obtained values in each model are very close to the experimental data. The best values found of R^2 are 0.9308 and 0.86558 for testing datasets in the RBF and MLP neural models respectively in order to predict CO emissions.

5. Conclusions

In this work, artificial neural networks (ANN) are constructed in order to predict the carbon monoxide engine emission of a gasoline engine. The CO emission is predicted in terms of four operating parameters of the engine. The architectures of RBF and MLP networks with smaller mean absolute percentage error (MAPE) are chosen and the correlation coefficient R^2 calculated. The correlation coefficient obtained with RBF neural network is 0.9306, this is greater than the obtained with MLP network, $R^2 = 0.86558$. Therefore, the RBF neural network is more suitable to predict CO emission than MLP neural network for the studied gasoline engine and operating parameters considered.

REFERENCES

- Ádám Bárdos, Huba Németh, (2017) Model development for intake gas composition controller design for commercial vehicle diesel engines with HP-EGR and exhaust throttling, *Mechatronics*, vol. 44 pp. 6–13.
- Guerrier M., and Cawsey P. (2004) “The development of model based methodologies for gasoline IC engine calibration”, *SAE paper*, No. 2004-01-1466.
- Hao Zhou, Jia Pei Zhao, Li Gang Zheng, Chun Lin Wang, Ke Fa Cen, (2012). Modeling NOx emissions from coal-fired utility boilers using support vector regression with ant colony optimization, *Engineering Applications of Artificial Intelligence*, vol. 25, pp. 147–158.
- Harisankar Bendu, B.B.V.L. Deepak, S. Murugan, (2016) Application of GRNN for the prediction of performance and exhaust emissions in HCCI engine using ethanol, *Energy Conversion and Management*. Vol. 122, pp. 165–173.
- Kiani M. K., Ghobadian B., Tavakoli T., Nikbakht A. M. and Najafi G. (2010) Application of artificial neural networks for the prediction of performance and exhaust emissions in SI engine using ethanol-gasoline blends, *Energy*, Vol. 35, No. 1, pp. 65-69.
- Kim H. and Sung N. (2001) “Multidimensional engine modeling: NO and soot emissions in a diesel engine with exhaust gas recirculation”, *Journal of Mechanical Science and Technology*, Vol. 15, No. 8, pp. 1196-1204.
- Martínez-Morales José D., Elvia Palacios, G. A. Velazquez-Carrillo, (2013) “Wavelet Neural Networks for Predicting Engine Emissions”, *Procedia Technology*, Vol. 7 pp. 328-335.
- Martínez-Morales José D., Elvia R. Hernández-Palacios, José M. Romo-Orozco, Gustavo Gallegos-Fonseca, (2014) “Comparación de desempeño de las redes RBF y LOLIMOT para modelar las emisiones de NOx de un motor de combustión interna”, *Congreso Latinoamericano de Control Automático*, Cancún, Quintana Roo, México.
- Mohammadhassania J., Dadvanda A., Khalilarya Sh., Solimanpur M., (2015) Prediction and reduction of diesel engine emissions using a combined ANN-ACO method, *Applied Soft Computing* vol. 34, pp. 139–150.
- Pitsch H., Barths H. and Peters N., (1996) “Three-Dimensional Modeling of NOx and Soot Formation in Di-Diesel Engines Using Detailed Chemistry Based on the Interactive Flamelet Approach”, *SAE Technical Paper*, No. 962057.
- Rakopoulos C., Antonopoulos K., Rakopoulos D. and Hountalas D. (2008) “Multi-zone modeling of combustion and emissions formation in DI diesel engine operating on ethanol–diesel fuel blends”, *Energy Conversion and Management*, Vol. 49, Num 4, pp. 625-643.
- Simpson P. (1990) Artificial neural systems: foundations, paradigms, applications and implementations, *Pergamon Press*, New York.
- Thompson G.J., Atkinson C.M., Clark N.N., Long T.W., and Hanzevack E. (2000) “Neural network Modelling of the Emissions and Performance of a Heavy-Duty Diesel Engine”, *In Proc. Instn. Mech. Engineers. Part D: J. Automobile Eng.* No. 214, pp. 111-126.
- Yiran Shi, Ding-Li Yu, Yantao Tian, Yaowu Shi, (2015), Air–fuel ratio prediction and NMPC for SI engines with modified Volterra model and RBF network, *Engineering Applications of Artificial Intelligence*, vol. 45, pp. 313–324.